RSC Advances

ROYAL SOCIETY OF CHEMISTRY

www.rsc.org/advances

Journal Name

ARTICLE

Fluorescent Organic Nanoparticles (FONs) for selective recognition of Al3+: Application to bio-imaging for bacterial sample

Carlos Alberto Huerta-Aguilar[a], Pushap Raj[b], Pandiyan Thangarasu[a]*, Narinder Singh[b]

Received 00th January 20xx,
Accepted 00th January 20xx

DOI: 10.1039/x0xx00000x

www.rsc.org/

The development of a novel chemo-sensor for the detection of Al^{3+} with high sensitivity in aqueous solution is widely considered an important research goal because of the importance of such probes in medicine, living systems and the environment. In this work, we describe a new fluorescent probe, a Schiff's base N,N'-propylenebis(salicylimine) (salpn) as fluorescent organic nanoparticles for Al^{3+}. The study shows that salpn detects Al^{3+} with the detection limit as low as 1.24 x 10^{-3} mM, indicating that the chemo-sensor has high sensitivity in aqueous medium, and the fluorescence intensity increases with the increasing Al^{3+} concentration in the presence of the salpn-ONPs which act as chemo-sensors. The interference of common coexistent metal ions such as Mn^{2+}, Mg^{2+}, Co^{2+}, , Fe^{3+}, Ni^{2+}, Zn^{2+}, Sr^{2+}, Ag^{+}, Sm^{3+}, Al^{3+}, Cd^{2+}, Ba^{2+}, Na^{+} and K^{+} was tested, showing that salpn-ONPs efficiently detect Al^{3+} ions with small interference from Cu^{2+} and Cr^{3+}. Finally, the efficiency of salpn to as a fluorescent probe for Al ion in living systems was evaluated in Gram-negative and Gram positive bacteria, and con-focal laser scanning microscopy confirms its utility that this chemo-sensor efficiently detects Al^{3+} ion in *Staphylococcus aureus* enclosed by a single membrane.

Introduction

The development of highly selective new fluorescent sensors for the detection of various metal ions or anions is essential for various biologically and environmentally important species[1-4]. Although analytical techniques as atomic absorption spectroscopy, colorimetric assays, spectrophotometry and voltammetry can effectively detect and quantify metal ions, these methods are either time consuming procedures or use sophisticated instrumentation; however, spectro-fluorescence has high sensitivity, selectivity, rapidity and an easy operational procedure[5-7]. Sensors based on changes in fluorescence induced by chemical species are highly sensitive, rapid, simple and there is real-time monitoring of the fluorescence, and they are able to detect numerous metal ions in biological samples[8-13] as follows: Ca(II) [14], Mg(II) [15-17], Pb(II) [18-20], Cd(II) [21-23], Al(III) [24-27], Cr(III) [28-29], Hg(II)[30-34], Fe(II) [35], Co (II) [36-37], Ni(II) [38-39], Zn(II) [40-46], Cu(II) [47-49], Ag(I)[50-51], Mn(II)[52]; rare earth metal ions[53-56].

Aluminum ion is generally employed to treat wastewater through co-precipitation or by coagulation process; however, its presence in water is toxic to biological species. For example, the presence of Al^{3+} ion in drinking water can cause damage to certain human tissues and cells, and produce Alzheimer's and Parkinson´s diseases and amyotrophiclateral sclerosis[57-61]. Thus, the detection of Al^{3+} in aqueous medium is important in order to minimize its effect on human health; yet the detection of aqueous Al^{3+} ion is generally difficult when compared with those for other metal ions due to its poor coordination ability, strong hydration ability, and the lack of suitable spectroscopic transitions.[62-64]

The following chemo-sensors have recently been used for the detection of Al^{3+}: 7-methoxychromone-3-carbaldehyde-((2-benzothiazolylthio)acetyl) hydrazone[7] in ethanol, 1-(2-pyridylazo)-2-naphthol[24] in methanol, N'-(4-diethylamino-2-hydroxybenzylidene)- 2-hydroxy-benzohydrazide[64] in CH_3CN/H_2O, 1-(2-hydroxy-5-methylphenylimino)- naphthalen-2-ol[65] in solvent mixture (water: methanol 1:9), 3,5-bis((E)-(2-hydroxyphenylimino)methyl)-4-hydroxybenzoate[66] in methanol, 8-formyl-7-hydroxyl-4-methyl coumarin–(2´-methylquinoline-4-formyl) hydrazone[67] in ethanol, 2-((E)-(2-((E)-2-hydroxybenzylidene-amino)phenylimino)methyl)phenol[68] in methanol, 2-chloronicotin- aldehyde functionalized rhodamine B

[a] Facultad de Química, Universidad Nacional Autónoma de México (UNAM), Ciudad Universitaria, Coyoacán 04510, México D. F., México.
[b] Department of Chemistry, Indian Institute of Technology (IIT), Ropar, India

† Footnotes relating to the title and/or authors should appear here.
Electronic Supplementary Information (ESI) available: [details of any supplementary information available should be included here]. See DOI: 10.1039/x0xx00000x

derivative[69] in CH_3CN, N,N´-bis(2-hydroxy-1-naphthaldehyde)-l,2-phenylenediamine[70] in DMF, 4-(8-hydroxyquinolin-7-yl)methylene-imino-1-phenyl-2,3-dimethyl-5-pyzole[71] in mixture of methanol:water. Thus most of the chemo-sensors are suitable only in non-aqueous medium (methanol, ethanol, or DMF). The detection of Al ion in 100% aqueous in the literature is limited, yet it is essential for real samples; moreover, although these sensors efficiently detect the metal ion, their applicability to real samples has not been studied, and there are only limited reports on Schiff base-type Al^{3+} sensors which are being used for bioimaging rare[64, 72-74]. The ability of bio-sensing molecules to selectively monitor guest species in living systems is important in biological applications. In the present work, salpn-ONPs have been found to selectively detect Al^{3+} ion at low detection limit (ppm level), and the receptor has been applied to real sample like *Staphylococcus aureus* and *Salmonella typhi* for the measurements of Al^{3+} ion..

Results and discussion

The organic nanoparticles have been fabricated through a re-precipitation method. The organic ligand dissolved in THF was injected into doubly distilled water at room temperature. The resulting solution was sonicated for 30 min in order to form stable nanoparticles. The formation and stability of organic nanoparticle was monitored by DLS and TEM techniques, and the results show that the particles have hydrodynamic radius of 100 ± 2 nm (see Fig.1); this is consistent with TEM studies that organic nanoparticles are of spherical shape with size of 100 nm (see Fig. S6). Both DLS and TEM data match with each other, confirming their stability in aqueous medium.

Fig. 1. DLS analyses of salpn-ONPs (0.01 mM) nanomaterials in water dispersion

The absorption and emission spectra of salpn and salpn-ONPs were analyzed in order to see the spectral difference between ligand and its organic nanoparticles (Fig. 2). In the UV-Vis spectra, a peak around 400 nm was observed, corresponding to the $\pi \rightarrow \pi^*$ transitions originating from the aromatic rings of the ligand, although there was a slight blue shift from 400 to 390 nm for salpn ONPs.

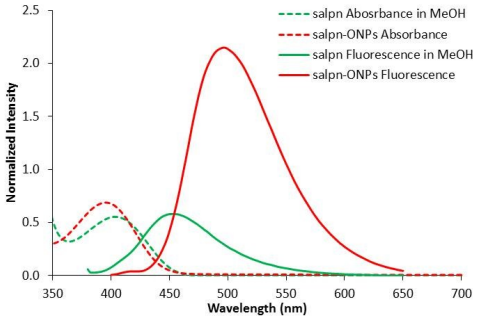

Fig. 2. Fluorescence and absorbance spectra of salpn in MeOH [0.1 mM] and ONPs suspension [0.1 mM].

In the fluorescence emission spectra, a significant spectral change was observed for salpn -ONPs compared to salpn when they were excited from 350 to 405 nm with a maximum wavelength of 365 nm. The fluorescence emission peak was observed around 460 nm for PBS**,** while the intensity of the peak was enhanced to around 510 nm for the ONPs due to the formation of J-type aggregates, agreeing with the supra-molecular self-organization typically found in organic nanoparticles. This type of interaction also leads to a redshift and broadening of the emission peaks.

Metal recognition binding tests

The selective recognition of different metal ions of salpn-ONPs was tested, and the different binding tests were performed for several anionic and cationic species. The binding test for anions in the form of *tetra-butyl* ammonium salts (F^-, I^-, Cl^-, Br^-, SO_4^-, ClO_4^-, COO^- and PO_4^-) was analyzed, and there are no emission spectral responses, so salpn-ONPs are not suitable for anion detection. Yet, for the metal binding test was carried out for sixteen different metallic ions in the form of nitrate salts (Mn^{2+}, Mg^{2+}, Cu^{2+}, Co^{2+}, Cr^{3+}, Fe^{3+}, Ni^{2+}, Zn^{2+}, Sr^{2+}, Ag^+, Sm^{3+}, Al^{3+}, Cd^{2+}, Ba^{2+}, Na^+ and K^+), and the ligand selectively detects Al^{3+} ion. In the experiment, each solution of the metal ion (50 µL, 0.1 mM) was added to salpn-ONPs (3.0 mL, 0.15 mM) suspended in water, and then the fluorescence emission (360-750 nm) was measured. Chemo-sensor salpn-ONPs were exited at 365 nm and the corresponding fluorescent emission signal was observed at 490 nm. There is a considerable increase in the fluorescence intensity for Al^{3+} compared to other cations, so salpn-ONPs are suitable for specific recognition of Al^{3+} ion (see Fig. 3).

Hydrated aluminium salts will be hydrolyzed to form hydroxylated aluminium compounds even with small amounts of moisture, and the

interaction of OH^- and H_2O (hard base) with hard-acid Al^{3+} makes it easier to form the Al^{3+} complex, so the Al ion may be chelated by the counter anion or solvent in order to satisfy the need of six-coordination. The organic nano-particles of salpn-ONPS are insoluble (colloid nature) in water, and their UV visible spectra in methanol show that there is no spectral change in both solvents. This confirms that hydrolysis of the ligand does not take place in the water medium. Moreover, if the ligand were to undergo hydrolysis, the fluorescence intensity would be expected to decrease or disappear due to the loss of conjugation.

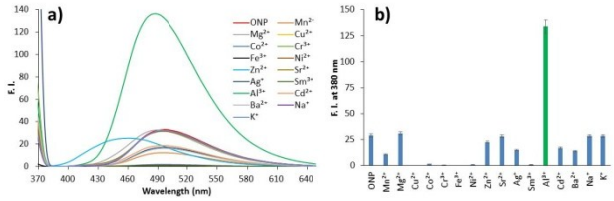

Fig.3. Metal binding test for fluorescence of salpn-ONPs [0.1 mM] in the presence of different metal ions in aqueous solution [10.0 µM). a) Fluorescence scanning upon addition of metal salts; b) comparison of fluorescence intensity at 380 nm.

Competitive binding analysis

The binding selectivity of salpn-ONPs with Al^{3+} was analyzed through fluorescence study in order to understand a possible interference of other metal ions. To the solution of salpn-ONPs (0.1 mM, 30 mL) /Al^{3+} (100.0 mM, 30 µL), different metal ions (30.0 µL, 100.0 mM) were added in such a way that the final concentration was 16.0 mM. The resulting solution mixture was stirred for 15 min and kept for 5 min. to reach equilibrium, and then the fluorescence emission was measured in the visible region after excitation at 365 nm. The results show that there is a small interference from Cu^{2+} and Cr^{3+} ions during the recognition of Al^{3+} through salpn-ONPs (Fig. 4) because the PBS-ligand can also bind with other metal ions of similar chemical nature (ionic radius: Cr^{3+} (0.73 Å) and Cu^{2+} (0.73 Å). The metal ions with *d* orbitals can coordinate with salpn in a similar manner and can interfere with the fluorescence signal originated from Al^{3+}/ONPs. However, there is no significant interference from Ag^+ (1.29 Å) or Cd^{2+} (1.09 Å) in the fluorescence because of their different acid-base chemistry.

The possible interference of other metal ions in the recognition of Al^{3+} by salpn-ONPs was analyzed by performing a set of interference experiments. In this case, salpn-ONPs suspension (30 mL, 0.1 mM) was mixed with 30.0 µL of Al^{3+} (100 mM), and the fluorescence intensity was measured for the resulting solution. With this spectral reference, a battery of tubes was prepared, each one containing 30.0 µL of one of the metal ions to be tested, and to these tubes 3.0 mL of salpn-ONPs (0.1 mM) and 30.0 µL of Al^{3+} were added

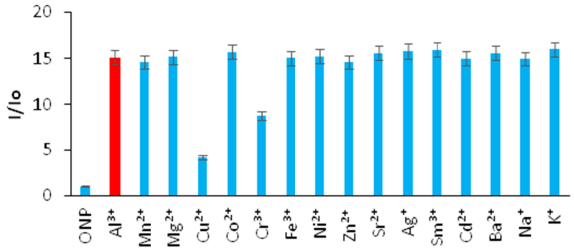

Fig.4. Interference binding test for recognition of Al^{3+} [10.0 µm] through salpn-ONPs 99[0.1 mM]

Titration studies salpn-ONPs against Al^{3+} ions

Titration analysis was performed in order to study the binding selectivity of salpn-ONPs with Al^{3+} ions. The fluorescent emission intensity was measured for each subsequent addition of Al^{3+}ions (0.0 to 0.45 mM) to salpn-ONPs (5.0 mL, 0.1 mM), and the peak intensity increased with increasing concentration of Al^{3+} in the ONPs (Fig. 5). Hence it was concluded that the fluorescence emission around 490 nm increases linearly with an increase of Al^{3+}concentration from 0.0 mM up to 0.1 mM. Above 0.1 mM, the changes in fluorescence after each addition decreased and after 3.0 mM concentration they become negligible. The results suggest that salpn-ONPs perform as chemo-sensors in recognizing Al^{3+} in aqueous solution. It appears that photo induced electron transfer (PET) occurs in the salpn-ONPs when the fluorophore is excited. i.e., an electron is transferred from the HOMO (donor) to the low-lying HOMO of the acceptor (fluorophore), causing quenching in fluorescence emission. However, when Al^{3+} is added to ONPs, metal ions bind with the salpn-ONPs moiety (recognition) and this causes the lowering of the receptor HOMO energy, thus inhibiting the photo-induced electron transfer from HOMO (donor) to fluorophore, and enhancing the fluorescence emission.

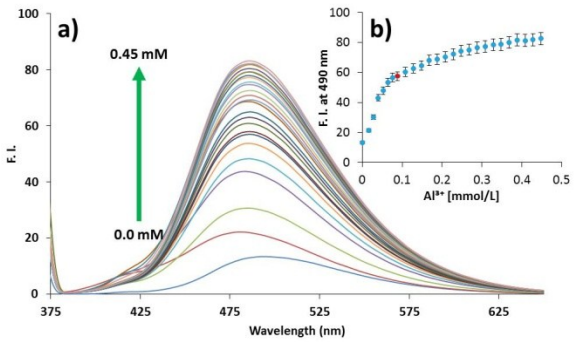

Fig.5. Titration of Al^{3+} (0.0 to 0.45 mM) in aqueous solution in presence of salpn-ONPs [0.1 mM]. a) Changes in fluorescence upon successive addition of Al^{3+} ions; b) Titration profile of fluorescence.

It appears that Photoinduced Electron Transfer (PET)[75-76] is operating in the sensor salpn-ONPS i.e., electron transfer is blocked when the receptor is coordinated to Al ion (the inhibition of PET process from the receptor to the fluorophore), enhancing the fluorescence intensity (scheme 1). This means that when irradiated by light, an electron of the donor highest occupied molecular orbital (HOMO) is excited to the lowest fluorophore unoccupied molecular orbital (LUMO), so CH=N- transfers an electron of HOMO to HOMO of the fluorophore, and =N- occupies the ground state of the fluorophore. Then the electron cannot transit back directly to the original ground-state, and the emission of the fluorophore is weakened. In the presence of Al^{3+}, which binds with electron donating sites of ligand, the lone electron pair of the =N- is lowered underneath the HOMO of the fluorophore. PET process inhibition then occurs with subsequent fluorescence enhancement and chelation enhanced fluorescence (CHEF). The high selectivity of receptor towards Al^{3+}can be explained by considering the high ionic potential and the high charge density of the Al^{3+}. The smaller radius of Al^{3+} allows suitable coordination environment of the chemosensor and the larger charge density allows strong coordination interaction between the receptor and Al^{3+}. The observed fluorescent intensity increment of salpn ONPS in the presence of Al^{3+} may be attributed to chelation-enhanced fluorescence (CHEF) of the receptor after binding with Al^{3+} imposed by the rigidity of the system. CHEF is one of the most widely applied mechanisms for fluorescent cation sensing. The fluorescence intensity of the fluorophore is significantly reduced in the absence of Al ion , due to photoinduced electron transfer (PET), but for its presence, PET[98-99] is prevented , leading to an enhanced fluorescence intensity due to rigid chelated complex formation. There are only a few reports for the detection of these ions using organic nanoparticles[77-83] which bind by weak intermolecular forces (van der Waals type) in organic molecular crystals, thereby affecting their electronic and optical properties [84 85-86 87].

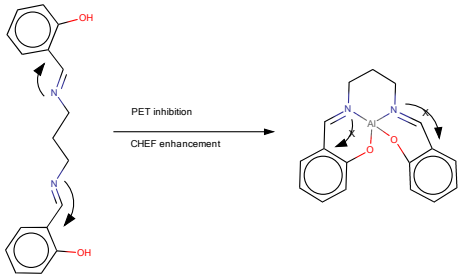

Scheme 1. Illustration of chelation-enhanced fluorescence (CHEF) of the receptor after binding with Al^{3+}.

pH effect. To check the effectiveness of the salpn-ONPs, the emission spectra were recorded in the range of pH 3-10. The fluorescence intensity increases with the decreasing pH (from neutral to acidic, pH 7-3), probably due to the inhibition of PET mechanism (see Fig. S7). However, the fluorescence intensity remains same in the range of pH 5-10, confirming that the sensor performs in the physiological range. The enhancement of fluorescent emission from [Al^{3+}/salpn-ONPs] (due to inhibition of PET mechanism) is approximately the same that observed for salpns-ONPs in acidic pH, confirming the involvement of PET mechanism for the enhancement of fluorescence[88-90].

Stoichiometry Determination. Job's method was employed to determine the stoichiometry of the reaction between salpn-ONPs and Al^{3+} ions (Fig. 6). In the study, the fluorescence intensity increases proportionally up to ~1.0 equivalents during the addition of Al^{3+}ions to ONPs at a ratio [Al^{3+}: salpn-ONPs] of 1: 1. In order to confirm these results, complementary FTIR and NMR analyses were performed by obtaining the spectra of the complex at different salpn:Al^{3+} ratios (1:2, 1:1 and 2:1 respectively). These results agree with DFT calculations and show there is formed a pseudo cavity between the two aromatic centers of the salpn molecule that allows the interaction with Al^{3+} ions.

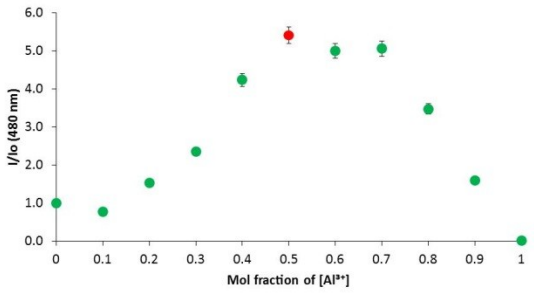

Fig.6. Job's plot for the determination of stoichiometry between salpn ONPs and Al^{3+} ions in aqueous solution.

From ^{1}H NMR analysis of the [salpn]Al^{3+} complex (Fig. 7), a certain amount of the complex was prepared in deuterated methanol (CD_3OD) and its spectra were recorded. It was found that most of the signals previously identified were split as usual in organometallic complexes, which suggests that protons are now found in two different environments.

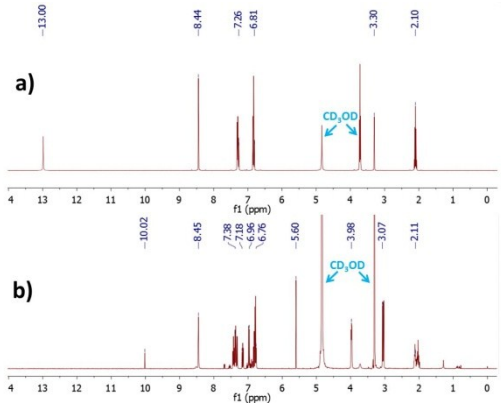

Fig.7. Comparison of ^{1}H NMR spectra of salpn (a) and [salpn]Al^{3+} (b) in CD_3OD for determination of complex structure

In case of aromatic protons, the splitting signals led to multiplets which can be observed at δ= 6.76, 6.96, 7.18 and 7.38 ppm. Moreover, new peaks were found that confirm the formation of a new complex. The doublet at δ=3.98 ppm and the singlet at δ=5.60 ppm suggest the presence of a methanol molecule attached to the Al^{3+} ion and at the same time, the absence of the OH signal confirms the coordination of salpn oxygen's with the metallic atom. The final confirmation of the complex formation was the presence of a new peak at δ=10.31 ppm that was attributed to HNO_3 molecules formed after interaction with salpn molecule according to scheme 2:

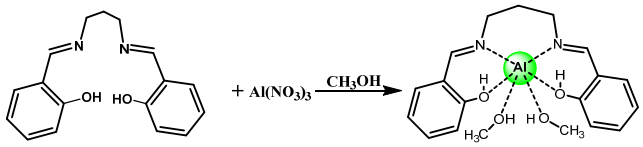

Scheme 2. Complex formation of [salpn]Al^{3+} in methanol

The geometry of the salpn molecule as well as the salpn-Al^{3+} complex were optimized and frequency calculations were executed, in both cases using 6-311G (d, p)/B3LYP basis set because of its ability to calculate both organic and organometallic complexes. The optimized structures of the ligand and the Al^{3+} complex are shown in Fig. 8. The structure of the salpn-Al^{3+} complex corresponds to 1:1 stoichiometry based on the results obtained from NMR and FTIR complexation analyses; moreover, this structure agrees with previous reports dealing with aluminum complexes[91].

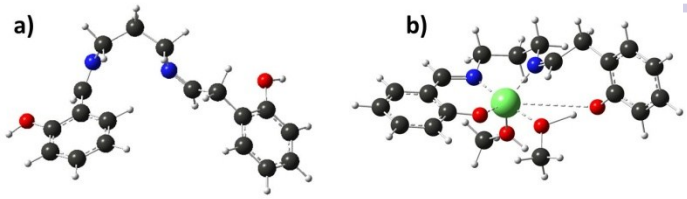

Fig.8. DFT optimized geometry through 6-31G (d, p) for a) salpn and b) salpn-Al^{3+}.

After optimizing inputs, theoretical UV-Vis spectra of salpn and salpn-Al^{3+} complex were calculated through Time Dependent (TD-DFT) calculations (Fig. 9). In order to get profiles closer to the experimental results, a polarizable continuum model (IEF-PCM) was used by employing water as the solvent[92-93].

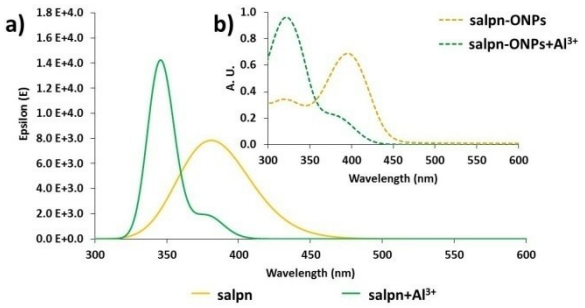

Fig.9. Theoretical and experimental UV-Vis absorption profiles of chemosensors and Al^{3+} complex; a) DFT theoretical profiles obtained through 6-31G (d, p)/B3LYP and using water as solvent and b) experimental profiles obtained for salpn -ONPs in water.

Reorganization of Al^{3+} in biological samples. The fluorescent probe of salpn-ONPs against *Stapylococcus aureus* and *Salmonella typhi* were analyzed in order to demonstrate its potential application in biological systems. The cells were incubated with different substrates (see Table 1) at 36^{0}C for 36 hours in Muller Hinton broth.

Table 1. Treatments of *Stapylococcus aureus* and *Salmonella typhi* broths for recognition of Al^{3+} in aqueous media.

Sample	Bacteria	Fluorescence response
Control		-
salpn-ONPs		-
salpn-ONPs+Al^{3+}	*S. aureus*	+
salpn		-
salpn+Al		-
Control		-
salpn-ONPs		-
salpn-ONPs+Al^{3+}	*S. typhi*	-
salpn		-
salpn+Al		-

After the bacterial culture was completed, the cells were centrifuged at 3000 rpm for three minutes, washed with 1% Triton-X-100 solution, followed by distilled water twice. The cell count was performed by using hemocytometer, and the results show that the *S. aureus* grow about 0.9% faster than *S. typhi*. The pellet in the bottom of the entrifuge tube was recovered and analyzed through confocal microscopy with excitation at 405 nm and the emission was monitored between 420 and 540 nm.

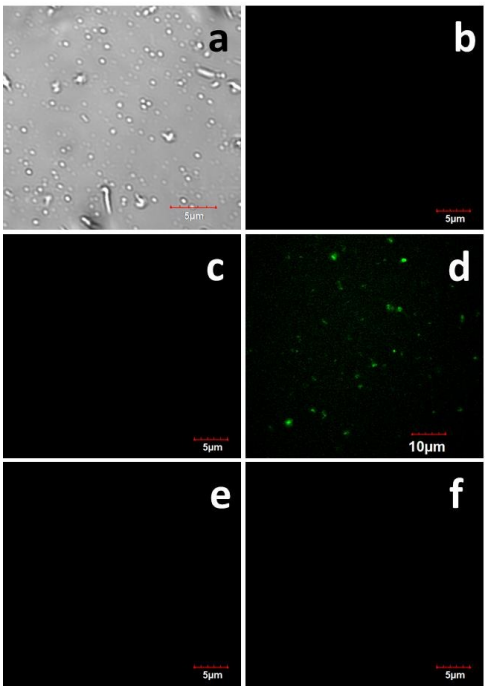

Fig.10. Recognition of Al^{3+} through bio-fluorescence *Staphylococcus aureus* treated with different combinations: a) *S. aureus* under visible light; b) control growth; c) *S. aureus* treated with salpn-ONPs (0.1 mM); d) *S. aureus* treated with salpn-ONPs (0.1 mM) and Al^{3+} (0.01mM); e) *S. aureus* treated with salpn (0.1 mM); f) *S. aureus* treated with salpn (0.1 mM) and Al^{3+} (0.01mM).

The confocal micrographs show that only for gram positive *Staphylococcus aureus,* fluorescence response was obtained when they grew in the presence of both analytes (salpn-ONPs-Al^{3+}) (Fig. 10) i.e., when salpn-ONPs/*S. aureus* cells were put in contact with an aqueous solution containing Al^{3+} [0.01 mM], it was possible to observe the fluorescent cells. However, for other combinations of samples, negative fluorescence response was resulted. This indicates that the aluminum complex of salpn-ONPs incorporates into the cytoplasm of the bacterium cell, and readily reacts with the compound present in the media.

For *Salmonella typhi*, there is no change in fluorescence response upon treatment with salpn-ONPs and Al^{3+} (Fig. S8 and S9). This behavior can be explained that *Staphylococcus aureus* is a gram positive bacteria with a thin cell wall which allows nanoparticles into the bacterium, while for gram negative bacteria, the presence of thick cell wall hinders the introduction of salpn-ONPs into the cell. This is consistent with the reported observation that the interaction of Schiff bases is stronger for gram positive than for gram negative bacteria[94].

In the SEM analysis, it has been found that salpn-ONPs were present within the bacterial cell (see Fig. S10), not on the cell surface, confirming the selectivity of aluminium complex in *S. aureus* through cellular uptake, and not by the cellular adherence. This indicates that salpn-ONPs can easily enter into cytoplasm of the cell and react with the compounds present in the medium as observed previously in that the Schiff base metal complexes interact strongly with gram positive bacteria rather than gram negative bacteria, incorporating the metal complex easily into the lipid membrane of the gram positive bacteria.[95-99]

Experimental

General remarks

All chemical reagents were purchased from Sigma Aldrich and used without further purification. The bacterial strains were obtained from the Strain Bank (WFCC/WDCM-100), Faculty of Chemistry, UNAM for cell culture, and maintained in Cysteine Tryptic Agar (CTA). Cysteine Tryptic Agar medium (CTA, BIOXON) for cell culture maintenance, Mueller Hinton (DIBICO) for inoculum dilution mixture.

Elemental analyses were carried out on a Fisons (Model EA 1108 CHNS). NMR (300 MHz Varian) and Mass Spectrometry (LECO Pegasus 4D) with a TOF analyzer were used to characterize the ligand. UV-Vis spectrophotometer (Perkin-Elmer Lambda 25) and

fluorescence spectrophotometer (F-96 Pro) were employed to analyze electronic and fluorescence properties of salpn-ONP as well as for the detection of metal ions. Confocal fluorescence imaging was performed on a Leica TCS SP5 laser scanning confocal microscope (Leica Microsystems, Wetzlar, Germany), with a blue diode laser (50 mW, lex=405 nm) and acquisition as xyz at a speed of 400 Hz.

Synthesis of N,N'-propylenebis(salicylimine) (salpn).

The ligand salpn was synthesized (scheme 3) as reported elsewhere[100-101]: To 2-hydroxybenzaldehyde (2.0 mmol, 244.0 mg) dissolved in methanol, 1,3-diaminopropane (1.0 mmol, 74.0 mg) was slowly added under vigorous stirring, and then the resulting mixture was stirred for 2.0 hours. The color of the solution changed from colorless to bright yellow, and yields a yellow product which was filtered and washed three times with ethanol. The compound obtained was crystallized from ethanol. Yield: 79.69 %; Elemental Analysis for salpn, Calc.: C, 72.32; H, 6.43; N, 9.92. Found: C, 72.430; H, 6.300 N, 10.210; S, 0.075. ^{1}H NMR (400 MHz, THF-d_8) δ 13.147 (s), 8.449 (s), 7.297 (m), 7.278 (m), 6.874 (m), 6.826 (m), 3.726 (t), 2.090 (m); ^{13}C NMR (101 MHz, THF-d_8) δ 165.99, 161.30, 131.74, 131.20, 119.00, 118.04, 116.45, 56.82, 31.93. GC-MS (*m/z* %): 282 [M^+, $C_{17}H_{18}N_2O_2$]; 162 (12.5%) $[C_{10}H_{12}NO]^+$; 148 (100.0%) $[C_9H_{10}NO]^+$; 134 (85.2 %) $[C_8H_8NO]^+$; 107 (49.6 %) $[C_7H_7O]^+$; 77 (66.7 %) $[C_6H_5]^+$.

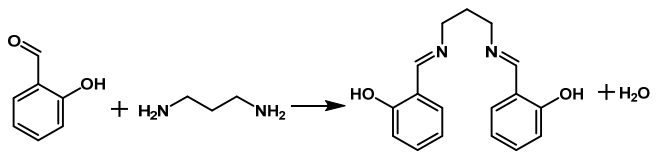

Scheme 3. Synthesis of salpn

Synthesized salpn was fully converted to organic nanoparticles (salpn-ONPs) through the re-precipitation method published elsewhere[102-103]. Ligand salpn (0.01 mmol, 2.82 mg) was dissolved in 1.0 mL of THF, and then it was then slowly injected through a micro syringe into 100 mL of deionized water under sonication to form suspension. The resulting mixture was further sonicated for 15 min. to yield a colloidal milky yellowish suspension of salpn-ONP (0.5 mM) with a final concentration of 0.1 mM of salpn -ONPs.

Computational studies

For the salpn-structure, a full optimization was performed by Density Functional Theory (DFT) using Gaussian'09 [104] at B3LYP with 6-311+G(d,p) basis set [105], and Polarizable Continuum Mode (IEF-PCM) was used to determine the effect of water as solvent. The structural data obtained were used as input to calculate Time-Dependent DFT (TD-DFT) [106-107]. To optimize the structure of [Al-salpn]$^{2+}$, B3LYP with LANLDZ basis set was employed, and then UV-visible spectrum and Density of States (DOS) diagrams were obtained through TD-DFT calculations. In the structure, two nitrogen and two oxygen atoms are coordinated with the Al^{3+} ion and their negative charge was detected by electrostatic potential analysis. The ligand (receptor) was found to coordinate efficiently with the metal ion (acceptor).

Cell culture study

The ability of salpn-ONPs to recognize metallic ions was tested by inoculating the molecule into *Staphylococcus aureus* and also *Salmonella typhi* bacterial cells suspended in Mueller Hinton broth[108]. Bacterial cells were obtained from a ceparium available at our institution. For each test, bacteria were inoculated into the broth and incubated at 36.0 °C for 36 hours before confocal microscopy analyses. The culture medium was taken in culture tubes protected with a plug. For inoculation, the microbes were dissolved in water and one drop of this suspension was added to each tube of a medium. The cultures were a clear solution (to the naked eye) at the beginning and with the growth of microbes, cloudiness appeared. After incubation, the bacterial content of each tube was recovered by centrifugation at 3000 rpm and washed with 1% Triton-X-100 solution followed by two times with doubly distilled water.

In the cell counting process, to the centrifuge tube containing S. aurous cell suspension (100 µl), trypan blue (100 µl) was added. The resulting mixture was first agitated to homogenize the suspension mixture, and then it was allowed to stand for 10 min. A small amount of trypan blue-cell suspension was carefully transferred to the chamber of hematocytometer and the cells were viewed by microscope, and were counted in each square of the grid. Similarly, the cell number of *S. typhi* was counted. The concentration of *S. aureus* was 18 x 10^4 cells/mL, and for *S. typhi*, it was 16 x 10^4 cells/mL. To maintain equal cell count, and also to fix the concentration of both bacteria, 0.12 mL of nutrient medium was added to 0.888 mL of S aurous suspension.

In the florescence microscopy, the respective bacterial cells were inoculated with different combination of salpn, salpn-ONPs and Al^{3+} at 36^0C at 36 hours (see Table S1). The growing bacteria were

washed with 1% Triton-X-100 solution, followed by distilled water twice. Finally, the samples were analyzed by confocal microscopy with excitation at 405 nm, and the emission was observed around 420-540 nm. To understand the selectivity of *S. aureus* with [salpn-ONPs+Al^{3+}] over S typhi, SEM analyses were performed. The bacteria were centrifuged, fixed with glutaraldehyde (2.5%) and then dehydrated with ethanol. Samples were then placed in SEM with Au coating for observation with 15.0 kV secondary electrons SEM (JEOL, JSM 5900-LV, Tokyo, Japan).

Conclusions

The prepared organic nanoparticles are well characterized by DLS and TEM, and the fluorescence probe has been analyzed, showing that salpn-ONPs explore as a fluorescence sensor for aluminum ions with little interference of copper and chromium. Moreover, this sensor recognizes the aluminum ions in biological sample such as *Staphylococcus aureus* bacterial cells. The confocal microscopy confirmed the detection of Al^{3+} ions in *Staphylococcus aureus* over *Salmonella typhi* bacterial cells.

Acknowledgements

The authors acknowledge the Dirección General de Asuntos de Personal Académico (Project PAPIIT No IN209616) for economic support, USAII, Faculty of Chemistry, UNAM for instrumental, DGSCA, UNAM for computation facilities. Carlos Alberto Huerta Aguilar thanks CONACyT for a scholarship.

Notes and references

1 V. K. Gupta, A. K. Jain, S. K. Shoora.,*Sens. Actuators B-Chem.,* **2015,** *219*, 218.

2 Q. Meng, R. Zhang, H. Jia, X. Gao, C. Wang, Y. Shi, A. V. Everest-Dass, Z. Zhang, *Talanta,* **2015,** *143*, 294.

3 N. Roy, A. Dutta, P. Mondal, P. C. Paul, T. S. Singh, *J. Lumin.,* **2015,** *165*, 167.

4 A. Bencini, V. Lippolis, *Coord. Chem. Rev.,* **2012,** *256*, 149.

5 Z.-C. Liao, Z.-Y. Yang, Y. Li, B.-D. Wang, Q.-X. Zhou, *Dyes Pigm.* **2013,** *97*, 124.

6 Y.-W. Liu, C.-H. Chen, A.-T. Wu, *Analyst,* **2012,** *137*, 5201.

7 C.-j. Liu, Z.-y. Yang, L. Fan, X.-l. Jin, J.-m. An, X.-Y. Cheng, B.-d. Wang, *J. Lumin.* **2015,** *158*, 172.

8 J.-A. Zhou, X.-L. Tang, J. Cheng, Z.-H. Ju, L.-Z. Yang, W.-S. Liu, C.-Y. Chen, D.-C. Bai, *Dalton Trans.,* **2012,** *41*, 10626.

9 C. Zhou, Y. Song, Y. Li, *RSC Adv,.* **2014,** *4*, 33614.

10 Y. Zhao, X.-B. Zhang, Z.-X. Han, L. Qiao, C.-Y. Li, L.-X. Jian, G.-L. Shen, R.-Q. Yu, *Anal. Chem.,* **2009,** *81*, 7022.

11 J. F. Zhang, S. Kim, J. H. Han, S.-J. Lee, T. Pradhan, Q. Y. Cao, S. J. Lee, C. Kang, J. S. Kim, *Org. Lett.,* **2011,** *13*, 5294.

12 C. Yu, L. Chen, J. Zhang, J. Li, P. Liu, W. Wang, B. Yan, *Talanta,* **2011,** *85*, 1627.

13 Y. Yang, C. Yin, F. Huo, Y. Zhang, J. Chao, *Sens. Actuators B-Chem.,* **2014,** *203*, 596.

14 J.-m. An, Z.-y. Yang, M.-h. Yan, T. Li, *J. Lumin.* **2013,** *139*, 79.

15 P. S. Hariharan, S. P. Anthony, *RSC Adv.,* **2014,** *4*, 41565.

16 P. S. Hariharan, N. Hari, S. P. Anthony, *Inorg. Chem. Commun.,* **2014,** *48*, 1.

17 J.-c. Qin, Z.-y. Yang, L. Fan, B.-d. Wang, *Spectrochim. Acta A,* **2015,** *140*, 21.

18 L. Guo, S. Hong, X. Lin, Z. Xie, G. Chen, *Sens. Actuators B-Chem.,* **2008,** *130*, 789.

19 K. C. Tayade, A. S. Kuwar, U. A. Fegade, H. Sharma, N. Singh, U. D. Patil, S. B. Attarde, *J. Fluoresc.,* **2014,** *24*, 19.

20 J. Wang, S. Chu, F. Kong, L. Luo, Y. Wang, Z. Zou, *Sens. Actuators B-Chem.,* **2010,** *150*, 25.

21 P. S. Hariharan, S. P. Anthony, *Anal. Chim. Acta,* **2014,** *848*, 74.

22 X.-J. Jiang, M. Li, H.-L. Lu, L.-H. Xu, H. Xu, S.-Q. Zang, M.-S. Tang, H.-W. Hou, T. C. W. Mak, *Inorg. Chem.,* **2014,** *53*, 12665.

23 C. Kar, S. Samanta, S. Goswami, A. Ramesh, G. Das, *Dalton Trans.,* **2015,** *44*, 4123.

24 V. K. Gupta, S. K. Shoora, L. K. Kumawat, A. K. Jain. *Sens. Actuators B-Chem.,* **2015,** *209*, 15.

25 V. K. Gupta, A. K. Singh, L. K. Kumawat, *Sens. Actuators B-Chem.,* **2014,** *195*, 98.

26 P.-J. Hung, J.-L. Chir, W. Ting, A.-T. Wu, *J. Lumin.,* **2015,** *158*, 371.

27 T.-J. Jia, W. Cao, X.-J. Zheng, L.-P. Jin, *Tetrahedron Lett.,* **2013,** *54*, 3471.

28 Y. J. Jang, Y. H. Yeon, H. Y. Yang, J. Y. Noh, I. H. Hwang, C. Kim, *Inorg. Chem. Commun.,* **2013,** *33*, 48.

29 Y. Yang, H. Xue, L. Chen, R. Sheng, X. Li, K. Li. *Chin. J. Chem.,* **2013,** *31*, 377.

30 S.-L. Kao, S.-P. Wu, *Sens. Actuators B-Chem.,* **2015,** *212*, 382.

31 K. Kaur, S. Chaudhary, S. Singh, S. K. Mehta, *Sci. Adv. Mater.,* **2014,** *6*, 970.

32 T.-H. Ma, A.-J. Zhang, M. Dong, Y.-M. Dong, Y. Peng, Y.-W. Wang, *J. Lumin.,* **2010,** *130*, 888.

33 J. Ni, B. Li, L. Zhang, H. Zhao, H. Jiang, *Sens. Actuators B-Chem.,* **2015,** *215*, 174.

34 M. Shellaiah, Y. C. Rajan, P. Balu, A. Murugan, *New J. Chem.,* **2015,** *39*, 2523.

35 C. Liu, Z. Yang, M. Yan, *J. Coord. Chem.* **2012,** *65*, 3845.

36 G. J. Park, Y. J. Na, H. Y. Jo, S. A. Lee, C. Kim, *Dalton Trans.,* **2014,** *43*, 6618.

37 J. Bu, H. Duan, X. Wang, T. Xu, X. Meng, D. Qin, *Res. Chem. Intermed.,* **2015,** *41*, 2767.

38 R. Kavitha, T. Stalin, *J. Lumin.,* **2015,** *158*, 313.

39 L. Wang, D. Ye, D. Cao, *Spectrochim. Acta A,* **2012,** *90*, 40.

40 V. K. Gupta, N. Mergu, A. K. Singh, *Sens. Actuators B-Chem.,* **2014,** *202*, 674.

41 V. K. Gupta, A. K. Singh, L. K. Kumawat, *Sens. Actuators B-Chem.,* **2014,** *204*, 507.

42 M. Hosseini, A. Ghafarloo, M. R. Ganjali, F. Faridbod, P. Norouzi, M. S. Niasari, *Sens. Actuators B-Chem.,* **2014,** *198*, 411.

43 M. Hosseini, Z. Vaezi, M. R. Ganjali, F. Faridbod, S. D. Abkenar, K. Alizadeh, M. Salavati-Niasari, *Spectrochim. Acta A,* **2010,** *75*, 978.

44 W. H. Hsieh, C.-F. Wan, D.-J. Liao, A.-T. Wu, *Tetrahedron Lett.* **2012,** *53*, 5848.

45 J.-H. Hu, J.-B. Li, J. Qi, Y. Sun, *Sens. Actuators B-Chem.,* **2015,** *208*, 581.

46 J. J. Lee, S. A. Lee, H. Kim, N. LeTuyen, I. Noh, C. Kim, *RSC Adv.,* **2015,** *5*, 41905.

47 Y. Ha, D. P. Murale, C. Yun, S. T. Manjare, H. Kim, J. Kwak, Y. S. Leea, D. G. Churchill, *Chem. Commun.,* **2015,** *51*, 6357.

48 J. Jayabharathi, V. Thanikachalam, M. Vennila, K. Jayamoorthy, *Spectrochim. Acta A,* **2012,** *96*, 677.

49 C. Kar, M. D. Adhikari, B. K. Datta, A. Ramesh, G. Das, *Sens. Actuators B-Chem.,* **2013,** *188*, 1132.

50 Q. Lin, Q. Yang, B. Sun, T. Wei, Y. Zhang, *Chin. J. Chem.,* **2014,** *32*, 1255.

51 T. Anand, G. Sivaraman, P. Anandh, D. Chellappa, S. Govindarajan, *Tetrahedron Lett,.* **2014,** *55*, 671.

52 P. S. Hariharan, S. P. Anthony, *Spectrochim. Acta A,* **2015,** *136*, 1658.

53 K. Guzow, M. Milewska, D. Wrolewski, A. Gieldon, W. Wiczk, *Tetrahedron,* **2004,** *60*, 11889.

54 M. Hosseini, M. R. Ganjali, B. Veismohammadi, S. Riahl, P. Norouzi, M. Salavati-Niasari, S. D. Abkenar, *Anal. Lett.,* **2009,** *42*, 1029.

55 Y. Hu, Q.-q. Li, H. Li, Q.-n. Guo, Y.-g. Lu, Z.-y. Li, *Dalton Trans.,* **2010,** *39*, 11344.

56 Z. Liang, Z. Liu, Y. Gao, *Tetrahedron Lett.,* **2007,** *48*, 3587.

57 D. R. Crapper, S. S. Krishnan, A. J. Dalton, *Science,* **1973,** *180*, 511.

58 P. Nayak, *Environ. Res.,* **2002,** *89*, 101.

59 J. R. Walton, *J. Inorg. Biochem.,* **2007,** *101*, 1275.

60 E. House, J. Collingwood, A. Khan, O. Korchazkina, G. Berthon, C. Exley, *J. Alzheimers Disease,* **2004,** *6*, 291.

61 C. Exley, L. Swarbrick, R. K. Gherardi, F.-J. Authier, *Medical Hypotheses,* **2009,** *72*, 135.

62 Y. Zhao, Z. Lin, H. Liao, C. Duan, Q. Meng, *Inorg. Chem. Commun.,* **2006,** *9*, 966.

63 R. McRae, P. Bagchi, S. Sumalekshmy, C. J. Fahrni, *Chem. Rev.,* **2009,** *109*, 4780.

64 Y. Jiang, L.-L. Sun, G.-Z. Ren, X. Niu, W.-z. Hu, Z.-Q. Hu, *Chemistryopen,* **2015,** *4*, 378.

65 S. Dey, S. Halder, A. Mukherjee, K. Ghosh, P. Roy, *Sen. Actuators B-Chem.,* **2015,** *215*, 196.

66 X.-P. Ye, S.-b. Sun, Y.-d. Li, L.-h. Zhi, W.-n. Wu, Y. Wang, *J. Lumin.,* **2014,** *155*, 180.

67 J.-c. Qin, T.-r. Li, B.-d. Wang, Z.-y. Yang, L. Fan, *Spectrochim. Acta A,* **2014,** *133*, 38.

68 S. K. Shoora, A. K. Jain, V. K. Gupta, *Sens. Actuators B-Chem.,* **2015,** *216*, 86.

69 J. W. Jeong, B. A. Rao, Y.-A. Son, *Sens. Actuators B-Chem.,* **2015,** *208*, 75.

70 D. Zhou, C. Sun, C. Chen, X. Cui, W. Li, *J. Mol. Struct.,* **2015,** *1079*, 315.

71 L. Fan, X.-h. Jiang, B.-d. Wang, Z.-y. Yang, *Sens.Actuators B-Chem.,* **2014,** *205*, 249.

72 S. Kim, J. Y. Noh, K. Y. Kim, J. H. Kim, H. K. Kang, S.-W. Nam, S. H. Kim, S. Park, C. Kim, J. Kim, *Inorg. Chem.,* **2012,** *51*, 3597.

73 W.-H. Ding, W. Cao, X.-J. Zheng, W.-J. Ding, J.-P. Qiao, L.-P. Jin, *Dalton Trans.,* **2014,** *43*, 6429.

74 H. M. Park, B. N. Oh, J. H. Kim, W. Qiong, I. H. Hwang, K.-D. Jung, C. Kim, J. Kim, *Tetrahedron Lett.,* **2011,** *52*, 5581.

75 N. R. Chereddy, K. Saranraj, A. K. Barui, C. R. Patra, V. J. Rao, S. Thennarasu, *RSC Adv.,* **2014,** *4*, 24324.

76 N. R. Chereddy, M. V. N. Raju, P. Nagaraju, V. R. Krishnaswamy, P. S. Korrapati, P. R. Bangal, V. J. Rao, *Analyst,* **2014,** *139*, 6352.

77 N. Kaur, S. Kaur, A. Kaur, P. Saluja, H. Sharma, A. Saini, N. Dhariwal, A. Singh, N. Singh, *J. Lumin.,* **2014,** *145*, 175.

78 V. K. Bhardwaj, H. Sharma, N. Kaur, N. Singh, *New J. Chem.,* **2013,** *37*, 4192.

79 V. K. Bhardwaj, H. Sharma, N. Singh, *Talanta,* **2014,** *129*, 198.

80 S. Chopra, J. Singh, H. Kaur, H. Singh, N. Singh, N. Kaur, *New J. Chem.,* **2015,** *39*, 3507.

81 J. Hou, L.-Y. Wang, D.-H. Li, X. Wu, *Tetrahedron Lett.,* **2011,** *52*, 2710.

82 H. Li, H. Yan, *J. Phys. Chem. C* **2009,** *113*, 7526.

83 F. Qu, J. a. Liu, H. Yan, L. Peng, H. Li, *Tetrahedron Lett.,* **2008,** *49*, 7438.

84 E. A. Silinsh, *Organic Molecular Crystals: Their Electronic States;* Springer-Verlag: Berlin, **1980**.

85 H. Kasai, Y. Yoshikawa, T. Seko, S. Okada, H. Oikawa, H. Mastuda, A. Watanabe, O. Ito, H. Toyotama, H. Nakanishi, *Mol. Cryst. Liq. Cryst. A,* **1997,** *294*, 173.

86 H. Kasai, H. Kamatani, S. Okada, H. Oikawa, H. Matsuda, H. Nakanishi, *Jpn. J. Appl. Phys 2.,* **1996,** *35*, L221.

87 H. B. Fu, J. N. Yao, *J. Am. Chem. Soc.,* **2001,** *123*, 1434.

88 A. P. de Silva, B. McCaughan, B. O. F. McKinney, M. Querol, *Dalton Trans.,* **2003,** 1902.

89 G. R. C. Hamilton, S. K. Sahoo, S. Kamila, N. Singh, N. Kaur, B. W. Hyland, J. F. Callan, *Chem. Soc. Rev.,* **2015,** *44*, 4415.

90 S. Das, M. Dutta, D. Da,. *Anal. Method,* **2013,** *5*, 6262.

91 M. J. Stanford, A. P. Dove, *Chem. Soc. Rev.,* **2010,** *39*, 486.

92 D. Jacquemin, E. A. Perpète, G. E. Scuseria, I. Ciofini, C. Adamo, *J. Chem. Theor. Comput.,* **2008,** *4*, 123.

93 D. Jacquemin, E. A. Perpète, G. Scalmani, M. J. Frisch, I. Ciofini, C. Adamo, *Chem. Phys. Lett.,* **2006,** *421*, 272.

94 S. Arulmurugan, H. P. Kavitha, R. Venkatraman, *Rasayan J Chem.,* **2010,** *3*, 385.

95 F. Li, J. G. Collins, F. R. Keene, *Chem. Soc. Rev.,* **2015,** *44*, 2529.

96 J. Devi, S. Devi, A. Kumar, *MedChemComm.,* **2016.**

97 M. Polivkova, M. Valova, J. Siegel, S. Rimpelova, T. Hubacek, O. Lyutakov, V. Svorcik, *RSC Adv.,* **2015,** *5*, 73767.

98 S. K. Samal, M. Dash, S. Van Vlierberghe, D. L. Kaplan, E. Chiellini, C. van Blitterswijk, L. Moroni, P. Dubruel, *Chem. Soc. Rev.,* **2012,** *41*, 7147.

99 M. Zampakou, S. Balala, F. Perdih, S. Kalogiannis, I. Turel, G. Psomas, *RSC Adv.,* **2015,** *5*, 11861.

100 F. Doğan, M. Ulusoy, Ö. Öztürk, İ. Kaya, B. Salih, *J. Thermal Anal. Calorimet.,* **2009,** *98*, 785.

101 S. K. Sahoo, S. E. Muthu, M. Baral, B. K. Kanungo, *Spectrochim. Acta A,* **2006,** *63*, 574.

102 S. K. Sahoo, R. K. Bera, M. Baral, B. K. Kanungo, *J. Photochem. Photobiol. A: Chem.,* **2007,** *188*, 298.

103 S. Chopra, J. Singh, N. Singh, N. Kaur, *Anal. Method,* **2014,** 9030.

104 M. J. Frisch, G. W. Trucks, H. B. Schlegel, G. E. Scuseria, M. A. Robb, J. R. Cheeseman, J. A. Jr. Montgomery, T. Vreven, K. N. Kudin, J. C. Burant, J. M. Millam, S. S. Iyengar, J. Tomasi, V. Barone, B. Mennucci, M. Cossi, G. Scalmani, N. Rega, G. A. Petersson, H. Nakatsuji, M. M. Hada, K. T. Ehara, R. Fukuda, J. Hasegawa, M. Ishida, T. Y. Honda, O. Kitao, H. Nakai, M. Klene, X. Li, J. E. Knox, H. P. Hratchian, J. B. Cross, C. Adamo, J. Jaramillo, R. Gomperts, R. E. Stratmann, O. Yazyev, A. J. Austin, R. Cammi, C. Pomelli, J. W. Ochterski, P. Y. Ayala, K. Morokuma, G. A. Voth, P. Salvador, J. J. Dannenberg, V. G. Zakrzewski, S. Dapprich, A. D. Daniels, M. C. Strain, O. Farkas, D. K. Malick, A. D. Rabuck, K. Raghavachari, J. B. Foresman, J. V. Ortiz, Q. Cui, A. G. Baboul, S. Clifford, J. Cioslowski, B. B. Stefanov, G. Liu, A. Liashenko, P. Piskorz, I. Komaromi, R. L. Martin, D. J. Fox, T. Keith, M. A. Al-Laham, C. Y. Peng, A. Nanayakkara, M. Challacombe, P. M. W. Gill, B. Johnson, W. Chen, M. W. Wong, C. Gonzalez, J. A. Pople *Gaussian 09, Gaussian Inc.* Wallingford, CT., **2004**,

105 N. Jayanthi, J. Cruz, T. Pandiyan, *Chem. Phys. Lett.,* **2008,** *455*, 64.

106 J. Autschbach, *Comprehen. Inorg. Chem.* || *Elements to Applications* **2013,** *9*, 407.

107 F. Furche, D. Rappoport, *Theor. Comput. Chem.,* **2005,** *16*, 93.

108 H. Sharma, N. Kaur, T. Pandiyan, N. Singh, *Sens. Actuators B: Chem.,* **2012,** *166–167*, 467.